Effects of CO_2 dilution and O_2 enrichment on non-premixed turbulent CH_4-air flames in a swirl burner

H. Zaidaoui[1], T. Boushaki[1,2,*], JC. Sautet[3], C. Chauveau[1], B. Sarh[1,2], I. Gökalp[1]

[1]ICARE CNRS, 1C Avenue de la Recherche Scientifique, 45071 Orléans, France
[2]University of Orleans, IUT - GTE, 45067 Orléans, France
[3]Normandie University, CORIA UMR 6614, 76801 Saint Etienne du Rouvray, France

*Corresponding author's contact information:

Dr. Toufik BOUSHAKI
ICARE, CNRS
1C, Avenue de la Recherche Scientifique, 45071 Orléans, France
E-mail address: toufik.boushaki@cnrs-orleans.fr

Abstract

Effects of oxygen enrichment and CO_2 dilution on the characteristics of non-premixed methane-air turbulent flames in a coaxial swirl burner are investigated in this paper. The work primarily focuses on pollutant emissions (NOx and CO), flame structure and stability investigations. The experiments are conducted using a 1m high, 0.5 m wide, 25 kW parallelepiped combustion chamber, cooled by outside water. The burner configuration consists of two concentric tubes in which a swirler is placed inside the annular part for air or air-O_2-CO_2 supply that can allow to the rotation of the oxidant. Fuel is injected radially from the central tube. OH* chemiluminescence measurements are performed to describe the structure and stability of the flame providing information on the flame lengths and lift-off heights. The measurements are conducted with the oxygen concentrations ranging from 21 % to 35 %, CO_2 concentrations ranging from 0 to 20%, swirl numbers ranging from 0.8 to 1.4 and global equivalence ratios ranging from 0.8 to 1. The lift-off heights, the fluctuations of the flame base, and the flame lengths are determined as a function of these parameters. The results show that oxygen enrichment stabilizes better the flame, promotes the formation of NO_X and CO_2, and decreases the formation of CO. The dilution by CO_2 changes significantly the flame shape and its behavior. The flame becomes longer, less intense and unstable. CO_2 dilution reduces considerably the flame temperature which obviously reduces the NOx formation, but it is observed that CO_2 and CO concentrations in the flue gases are increased.

Keywords: turbulent flame, swirling flame, oxygen enrichment, CO_2 dilution, pollutant emissions, OH chemiluminescence.

1. Introduction

The reduction of pollutant emissions and the optimization of combustion system performances necessitate the development of new combustion technologies and an efficient control of flow and flame stability in the combustion systems (e.g. furnaces, boilers, gas turbines). Controlling and optimizing combustion systems is a priority, not only to avoid combustion instabilities (Lieuwen and Zinn, 1998; Poinsot, 2017), but also to improve combustion systems, ensure the flame stabilization and reduce pollutant emissions (Ma, T. and Takeuchi, 2017; Telesca et al., 2017). The present work aims to investigate the effects of oxygen enrichment and CO_2 dilution on non-premixed turbulent flame stability and pollutant emissions (NOx and CO) in a swirl burner.

The swirling flames studied in this work are mainly used in low-NOx burners which is designed for boilers and industrial furnaces to reduce NOx emissions (Boushaki, Sautet, J.-C. and Labegorre, 2009; European commission 2006) and enhance flame stability (Jourdaine et al., 2016). The essential requirement of swirler design is to enhance the mixing of the fuel and oxidizer and hence improves flame stability. The major controlling parameter of flame stabilization is the central recirculation zone CRZ (Kim, M.-K. et al., 2013); its size and position vary with swirl intensity (Merlo et al., 2014). The choice of CH_4 as fuel in this work is based on the fact that natural gas (composed essentially of CH_4) is the most common fuel used today to operate gas turbines because of its lower pollutant emissions, compared to other types of fuels (Lashof and Ahuja, 1990; Abdul-Wahab et al., 2015). Jaramillo, Griffin and Matthews (2007) reported that natural gas emits 40% less CO_2 than coal combustion and 15% less than crude oil, for equivalent power output.

The use of oxygen enrichment in combustion systems induces higher flame temperatures and significantly improves thermal efficiency (Ding, M. G and Du, Z. 1995). Merlo et al. (2013) found that the addition of oxygen increases the flame temperature and improves flame

stability. Nemitallah and Habib (2013) studied the diffusion flame stability characteristics using both experiments and numerical techniques indicating that the flame stability is affected when the fraction of oxygen in the oxidizer is less than 25%. Rashwan et al. (2016) studied the oxy-combustion of partially premixed flames and reported that the better stability of flame was obtained with range of oxygen fraction from 29% to 40%. Jerzak and Kuźnia (2016) studied the impact of the swirl number as well as oxygen and carbon dioxide content in natural gas combustion in air on flame flashback and blow-off. Their results show that the most favorable stable combustion range was observed for an oxygen enrichment rate of 25% and a swirl number of 1.35.

Exhaust gas recirculation is a widely used technique, particularly in engines with the aim of reducing nitrogen oxides (Yu, B., Lee, S. and Lee, C.-E., 2015; Gotoh O et al. 1984). It consists in redirecting part of the combustion gases to the combustion chamber in order to dilute the mixture and decrease the combustion temperature, thereby reducing NOx. Several recent studies show that the effect of flue gas recirculation is dominated by addition of CO_2 (Wang, S. et al., 2016). Kim, T.H. et al. (2016) studied chemical and radiation effects on flame extinction and NOx formation in oxy-methane combustion diluted with CO_2. They confirmed that NOx formation was significantly reduced due to increased radiation heat loss and chemical effects of CO_2 addition. Results of Allouis and Chiariello (2016) show that CO_2 dilution decreases NOx emissions (up to 20 times) due to the lower furnace temperature at fixed oxygen concentration. Jerzak and Kuźnia (2016) confirmed that the addition of CO_2 to combustion atmosphere widens flame flashback limits, which is due to the reduction in laminar burning velocity. The results reported by Min and Baillot (2012) show a decrease in NOx by the addition of CO_2, but an increase in CO, which results in incomplete combustion. A recent study of Liu, F. et al. (2015) confirmed that carbon conversion and even soot volume fractions are lower in the CO_2-diluted flames which is mainly due to the additional chemical

effect of CO_2 at high pressures. The study of Wei et al. (2016) on the CO_2 effect on heat release characteristics of premixed laminar biogas/hydrogen flame showed that CO_2 addition influences heat release rate through its dilution/thermal and chemical effects. In addition, the dilution of fresh gas influences the reactivity of the flame, which can lead to stability problems. Therefore, it is important to investigate precisely the dilution effect on the combustion process. The experimental results of Oh and Noh (2014) indicated that the stabilization of non-premixed methane-oxygen flames weakened with increasing mole fraction of CO_2 in the oxidizer. Nada, Matsumoto and Noda (2014) studied the effect of CO_2 dilution on the lift-off height of turbulent diffusion flames. They concluded that the increase in the amount of CO_2 in the oxidizer leads to decrease flame velocity which induces an increase of the flame lift-off height.

The present paper investigates the effects of recirculation gases, CO_2 in particular, and O_2 enrichments on non-premixed turbulent flames stabilized by a swirl burner. This work is motivated both by EGR "Exhaust Gas Recirculation" applications and CO_2 capture applications. Indeed, the increase of CO_2 concentration by the EGR and O_2 enrichment improves the CO_2 capture efficiency (Favre, Bounaceur and Roizard, 2009). This study focuses on the flame stability through the determination of lift-off heights and flame length and also on pollutant emissions based on different burner parameters such as: the swirl number, the global equivalence ratio, and the fractions of O_2 and CO_2 in the mixture. The experiments are based on the OH chemiluminescence technique to visualize the flame, on gas analysis *in situ* by multigas analyzers, and on temperature measurements in the combustion chamber. The paper deals with the pollutant emissions produced by combustion, the structure and the flame stability issues. The novelties of the study lie in the new configuration of the developed burner and the nature of the results concerning oxygen enrichment and CO_2 dilution. The burner has a coaxial configuration, with the presence of a swirl, a radial

injection of the fuel through small holes, a turbulent regime, a non-premixed flame and the presence of a combustion chamber. However, it is a complex configuration, but it has practical applications and there is a lack of detailed studies of this type of installation. Oxygen enrichment (21 to 35%) and the dilution in CO_2 (to simulate the recirculation of the combustion products) are the main studied parameters. Two other parameters are also investigated: a geometric parameter throughout the swirl number, and a chemical parameter throughout the equivalence ratio. The quantification of the effects of these parameters on pollutant emissions (CO and NOx), the lift off heights and the flame lengths are investigated in this work. The configurations of the swirl burner, the description of the combustion chamber, the operating condition are presented in the subsequent section. The final section discusses the effects of CO_2 and O_2 additions on the flame features.

2. Experimental setup

2.1 .Combustion chamber, burner and operating conditions

Figure 1 illustrates the experimental facility used in this study. It includes: the combustion chamber with the elements from A1 to A6, the chemiluminescence system (B1 to B3) and the gas analyzers (C1 to C3).

The experiments are conducted in a square cross-section chamber (A1 in Figure 1) of 48×48 cm^2 and 1 m high which is operating at atmospheric pressure. Six windows (A5) are placed on each face of the chamber for allowing optical access to the entire length of the flame. The combustion chamber is coated inside by a refractory insulation with low thermal conductivity (between 0.06 W / (m.K) at 200 ° C and 0.17 W / (m.K) at 600 °C). The walls of the combustion chamber are externally cooled by water which is flowing in stainless steel tubes (A4). The chamber top is a 20 cm high convergent with a circular section of 10 cm diameter at the outlet which is connected to the extraction tube (A3).

The burner (A2 in Figure 1) is placed at the bottom of the chamber which allows the flame to develop vertically along the combustion chamber. Figure 2 shows a detailed schematic representation of the coaxial swirl burner, which consists of several elements. The central tube (12 mm internal diameter) is used to supply methane to the radial injector. This injector comprises of 8 holes with 3 mm diameter, evenly distributed along the perimeter which enables a radial injection of fuel near the burner outlet. The swirler is placed in the coaxial air tube -60mm away from the burner outlet. This position makes it possible to thermally protect the swirler without weakening the effect of the swirl along the tube. It contains 8 blades and their angular orientations depend on the required swirl number. Figure 3 illustrates the type of flames obtained from this swirl burner. The effects of oxygen enrichment and CO_2 dilution are shown with the swirl number of Sn=1.4. The flame is completely lifted, which induces a partial premixing of the reactants before they reach the reaction zone. Therefore, the combustion process may be changed from an initial non-premixed type to a partially premixed type by means of the design of burner.

The swirl number represents the ratio of the angular momentum flux G_Θ, to the axial momentum flux G_z times a characteristic distance of the radial dimension R. It is defined as follows:

$$S_n = \frac{G_\Theta}{R\, G_z} \qquad [1]$$

The geometrical swirl number S_n for the present configuration can be expressed as (Boushaki et al., 2017):

$$S_n = \frac{1}{1-\psi} \cdot \left(\frac{1}{2}\right) \cdot \frac{1-(R_h/R)^4}{1-(R_h/R)^2} \tan\alpha_0 \qquad [2]$$

where α_0 is the vane angle, ψ is the blockage factor and R and R_h are nozzle and vane pack hub radii respectively.

The operating parameters are defined as follow:

The oxygen content in the oxidizer (Ω) is the ratio of oxygen flow rate to the total flow rate (oxygen and nitrogen) expressed as:

$$\Omega = \frac{O_2}{O_2 + N_2} \quad [3]$$

The CO_2 content in the oxidizer is written as:

$$\%\ \text{vol}\ CO_2 = \frac{Qco_2}{Q_{air}} \quad [4]$$

The global equivalence ratio is designated by Φ and the swirl number designated by Sn. In the present work, the oxygen content in the oxidizer varies from 21% to 30%, the CO_2 content ranges from 0% to 20%. The global equivalence ratio varies from 0.8 to 1 and the swirl number ranges from 0.8 to 1.4. Table 1 shows the operating conditions of the study, including the equivalence ratio, the swirl number, the O_2 and CO_2 addition rates, flow rates of air, O_2, CO_2 and CH_4 and the bulk velocities of CH_4 and the total oxidant.

2.2. Chemiluminescence technique and gas analysis

The chemiluminescence OH* technique is used to study the spatial position of the flame reaction zones via a characterization of lift-off heights and flame lengths. This technique enables to detect the flame contours to estimate the lift-off heights and the top position of the flame. In high-temperature furnaces, the chemiluminescence of the C2*, CH* and CO_2* radicals can be emitted in the visible light range which can be overlapped with heat emissions in the visible range from hot refractory walls. Therefore, it is preferable to measure the chemiluminescence of OH* radical in UV region to overcome this parasitic thermal radiation (Honoré D. 2007). In addition, the OH* radical characterizes the flame reaction zones and is presented with sufficiently high concentration providing a good quality signal, in particular for oxy-fuel combustion and oxygen enrichment combustion. The emission of OH* radical is located in the wavelength range from 280 to 310 nm. The experimental setup of

chemiluminescence measurments consists of an ICCD camera (B1 in Figure 1, Princeton Instrument PI-MAX Gen II) with a UV Nikkor lens of 105 mm focal length (f / 4.5), a camera control device (B3) (Peltier cooling and synchronization system), an interference filter CG-UG-11-2X2-1.0 (Melles Griot), centred on 306 nm with a bandwidth of 20 nm, and a computer (B2) to acquire and save the images.

The concentrations of NOx, CO, CO_2, O_2 and SO_2 in the flue gases are measured using a HORIBA PG250 multi-gas analyser (C1 in Figure 1). Oxygen is detected by its paramagnetic property, NOx (NO + NO_2) is analysed by chemiluminescence technique, and CO, CO_2 and SO_2 are measured via infrared non-dispersive detectors. Combustion products are sampled by a PSP4000-HCT probe (C2) and transported via a transfer line (C3) heated at 180 °C to prevent condensation of water that could deteriorate gas analysis. The water vapour in the flue gas is subsequently removed by a cooling unit (pre-sampler PSS5) before it reaches the analyser which provides measurements on dry flue gases. The sampling probe is located on the central axis of the chamber at 1.2 m from the burner.

3. Results and discussions

3.1. Effects of oxygen enrichment

The purpose of this section is to describe the effect of oxygen enrichment, on non-premixed swirled turbulent flames, through direct observations as well as determination of lift-off heights and flame lengths from OH* chemiluminescence imaging. Note that the results considered in this part are without CO_2 or with a fixed CO_2 concentration in the oxidizer. Image acquisitions are performed using the WinView32 software, which allows the recording and viewing of images. This system is capable to control the gain, the duration of the camera intensification gate and the lens aperture to maintain a satisfactory signal/noise ratio to avoid the saturation of camera. The exposure time is fixed at 40 ms for each image. The sensor of the camera consists of a matrix with size of 1024 x 1024 pixels and the images are coded on

16 bits at the output. The measurement window is of 112x112 mm^2 with a spatial resolution of 9.2 pixels/mm. The acquisition is carried out over 300 images in order to ensure efficient statistical representation, and to allow the calculation of statistical parameters (converged average and standard deviation) during the image processing. A Matlab image processing program (thresholding, binarization, filtering and contour detection) was developed to extract lift-off heights and flame lengths and the corresponding standard deviations. An explanatory diagram for image processing is shown in Figure 4.

Figure 5 presents average images of OH* chemiluminescence for both cases, without enrichment (21% of O_2) and with O_2 enrichment (25% and 30% of O_2 in the oxidizer). The average images are obtained from 300 instantaneous images for each case. This average image is calculated by averaging pixel by pixel the light intensity using a program made by Matlab software. Regardless of O_2 enrichment, the images show two intense zones, on the left and right of the center image. This corresponds to the presence of reaction zones in the annular part of the burner downstream of the burner exit. The images show that the O_2 enrichment significantly affects the flame shape and behavior. Consequently, the flame becomes less voluminous and its base approaches the burner when the oxygen enrichment increases. However, it appears that oxygen enrichment enables to widen the range of flame stability of tested conditions of the burner, which is probably linked to an extension of the flammability limits of the CH_4 in oxygen enriched air mixtures.

The lift-off heights of flame with oxygen enrichment are presented in Figure 6. These results correspond to the case of a swirl number Sn=1.4, an equivalence ratio of Φ=0.8 and the presence of 10% (in vol.) of CO_2 in the oxidizer. The flame lift-off heights and its standard deviations (vertical bars) are determined from OH* images by using the method described in Figure 4. Lift-off height measurements show a slight decrease when the oxygen concentration is increased from 21% to 30%. Without oxygen enrichment, the flame occurs at 24.5 mm

from the burner outlet plane. With oxygen enrichment of 30%, the flame base occurs at 21 mm from the outlet of the burner, which represents a decrease of 12% in lift-off heights between 21% and 30% of oxygen enrichment. The presence of oxygen with reactants promotes the stability of flame that approaches the burner. This is due to the increase of the flame temperature as well as the flame velocity. These positive effects broaden the flame stabilization zones and improve its stability. The base of the flame fluctuates by about ±3mm with and without the oxygen enrichment, and this is probably due to CO_2 content in the oxidizer.

In Figure 7 the flame length (L_f) is plotted versus the oxygen enrichment in the case of Sn=1.4, Φ=0.8 and 10% of CO_2 content. The results show a decrease in flame lengths from the oxygen content increased from 21% to 27% with a stabilization thereafter (27% - 30%). For example, at 21% of oxygen, the flame length is 48mm, whereas with 27% of oxygen enrichment, the flame length is about 42mm, which represents a decrease of 11% of flame length from 21% to 27% of O_2 rate. It is noted that the fluctuation in flame length decreases with O_2 enrichment. Indeed, at 21% of O_2 the deviation of L_f is 4.5 mm, whereas at 27% the value is 2.5 mm. However, the oxygen air enrichment widens the range of flame stability over the studied burner, tends to stabilize the flame and shortens the flame length. The addition of oxygen increases the oxidation reaction rates, hence the decrease of the reaction zone size. Consequently, the flame becomes more compact, more intense and more stable.

3.2. Effects of CO_2 dilution

Figure 8 shows average images of OH* chemiluminescence for various CO_2 dilution rates (0%, 8% and 16%) with 21% of O_2 content, a swirl number of 1.4 and a global equivalence ratio of 0.8. The dilution of reactants by CO_2 influences significantly the flame characteristics. The images show that the increase of CO_2 content in the oxidizer changes the flame shape, the

intensity and the flame front position. The CO_2 addition tends to move the flame towards the burner and the flame becomes less intense, more stretched and leaner.

From the OH images, the flame heights as a function of CO_2 content in the oxidizer are determined and shown in Figure 9. These results concern the case with the swirl number of 1.4 and the equivalence ratio of 0.8. The content of CO_2 varies from 0 to 16% by volume relative to air. The results show that the lift-off height increases slightly at 2%vol of CO_2 content, and decreases considerably thereafter reached plateau level between 22 and 24 mm up to a CO2 content of 16%vol in the oxidizer. It can be seen in the average images in Figure 8 that the flame length increases and its width decreases by increasing the CO_2 content in the oxidizer. This is due to the modification of the reaction zone size by the dilution effect. This unexpected result is very important since the dilution by CO_2 seems not to affect the flame stability. It should be, however, mentioned that the base of the flame is modified with the addition of CO_2. It is not as wide and has less stabilization zone compared to the case without CO_2.

Figure 10 shows the influence of the CO_2 dilution on the flame length for a swirl number of 1.4 and a global equivalence ratio of 0.8. It is noted that the addition of CO_2 leads to an increase in the length of flame. For example, L_f = 48 mm without dilution case, and L_f = 60.5 mm in the case of 16% CO_2 dilution; this represents an increase of 21% of flame length. The fluctuations in the flame length are relatively high in particular with the increase of CO_2 content in the oxidizer.

3.3. NO_x and CO emissions

In this section, the pollutant emissions of NOx and CO with on oxygen enrichment and CO_2 dilution rates are analysed. Figure 11 shows NOx emissions as a function of oxygen enrichment for the three swirl numbers, Sn=0.8, 1.1 and 1.4 with an equivalence ratio of Φ=0.8. The results indicate that NOx emissions increase significantly with the oxygen

enrichment. This trend occurs for the three swirl numbers tested. Indeed, for the swirl number of 1.4, when the oxygen content in the oxidizer increases from 21% to 30%, the NOx level increases from 10 to 100 ppm, which represents a factor of 10. This evolution can be explained by the fact that the increase of flame temperature when the oxygen enrichment increases, promotes the formation of thermal NOx as also observed in other studies (Samaniego et al., 1998; Wu et al., 2010; Merlo et al., 2014). Note that the increase of temperature flame with O_2 enrichment is observed throughout the temperature of combustion products shown in Figure 13. Considering the swirl numbers effect, it is noted that the highest swirl number provides the lowest NOx content, especially for high O_2 fractions. The high swirl intensity increases the entrainment of combustion products which dilutes the reactants. This allows decreasing the flame temperature and thus reducing the NOx thermal production. In addition, with swirling flow, the mixing efficiency can be improved thus diminishing the possible hot spots in the mixture. However, the intensity of swirl must not be very strong because it induces a change of trend, as can be seen later.

Figure 12 illustrates the influence of CO_2 dilution on NOx emissions for the three swirl numbers 0.8, 1.1 and 1.4 at Φ=0.8. The results show that the formation of NOx decreases considerably by increasing the CO_2 content in the oxidizer. The same trend occurs for the three swirl numbers. For Sn=1.4, the NOx rate reduces from 8 to 2 ppm when the CO_2 is added in the reactants from 0 to 14%. It is interesting to note that at 14-16 % of CO_2 in the oxidizer, the flame remains stabilized as shown in Figure 8 and 9. However, this is a very notable result because the NOx emissions are reduced and the flame is stable even at high CO_2 dilutions. This is due to the reduction of reactant concentrations in the mixture, hence lowering the flame temperature as shown in Figure 13, which results in a decrease of NOx emissions as also reported in (Yap et al., 2008). As noted before, the highest swirl number exhibits relatively low NOx, except for higher CO_2 dilution in which the NOx values are

uniform for the three swirl numbers. However, over 8% of CO2 dilution, the NOx rate for Sn=1.4 (black curve) becomes slightly higher than the NOx rate for Sn=1.1. In this case, the difference in NOx emissions between Sn=1.1 and Sn=1.4 is very low (≈ 1 ppm), but it is repetitive. This result is explained by the presence of both parameters at the same time: the high dilution in CO_2 and the high intensity of swirl. The effect of this very strong dilution probably disturbs the mixing of the reactants and induces this behavior. It is noted that the swirl intensity affects the flow field and consequently the flame (Boushaki et al. 2007), in particular in the central recirculation zone (CRZ). In the same paper, it is showed that the NOx emissions are related to recirculation mass ratio that is measured by velocity fields. Another explanation relates to the mechanism of NOx formation. In this case, it is no longer thermal NOx which is reduced by the dilution, but maybe prompt NOx. The formation of prompt NOx is favored by a rich mixture, which can be caused locally by the high swirl intensity (despite the low global equivalence ratio) in our configuration. The value of swirl number must be limited to avoid any reverse effect of NOx emissions. The same results were found by the authors in (Boushaki et al. 2009). It was observed that there is a critical value of swirl intensity beyond which the NOx level may increase.

Figure 13 shows the evolution of exhaust gases temperature with oxygen enrichment and CO_2 dilution rates for three equivalence ratios of 0.8, 0.9 and 1, with a swirl number of 0.8. The results show that for different equivalence ratios, the increase of oxygen enrichment induces an increase in exhaust gas temperatures following the decrease of flame temperature. This favors the NOx emission as shown in Figure 11. The second graph of Figure 13 shows that the increase of CO_2 content decreases the exhaust gases temperature caused by the decrease of the flame temperature, which reduces the NOx emissions as found in Figure 12. For both cases, the temperature increases when the equivalence ratio approaches stoichiometry.

The influence of oxygen enrichment and CO_2 dilution on carbon monoxide formation is very significant. The CO measurements are carried out with different swirl numbers and different global equivalence ratios, for an oxygen concentration ranging from 21% to 35% by volume and CO_2 dilution ranging from 0% to 10% by volume. Figure 14 shows carbon monoxide emissions as a function of oxygen enrichment for three swirl numbers, 0.8, 1.1 and 1.4 with a global equivalence ratio of 0.8. The results show that the concentration of CO in the flue gases decreases significantly by increasing the oxygen content in the oxidizer. For 30% vol. of O_2 in the oxidizer, the CO concentration is almost zero (0 to 3 ppm). This reduction is due to the increase in oxidation reaction rates with O_2 enrichment, resulting in improved combustion (Merlo et al., 2014). However, the comparison of the three swirl numbers shows that the CO rate increases with the increase of swirl number for Φ=0.8. The result is a bit unexpected. This increase in CO is related to the high swirl number combined to lean regime, which can disturb the mixing and probably promotes the formation of CO. In the case of stoichiometric condition (Φ=1), the CO rate evolution is similar for the three swirl number as shown in Figure 17. These results show that the high dilution induced by the addition of CO_2 and the high swirl intensity does not systematically favor the mixing of reactants for all equivalence ratios. Therefore, even for CO emissions, the intensity of flow rotation should be limited to reduce CO emissions.

The effect of CO_2 dilution on CO concentrations in flue gases is shown in Figure 15 for three global equivalence ratios; 0.8, 0.9 and 1 and a swirl number of 0.8. The addition of CO_2 to the oxidizer increases significantly the CO content in flue gases. The increase in the equivalence ratio leads to a reduction in the CO emissions. For an equivalence ratio Φ=1, the concentration of CO is 1400 ppm, whereas for an equivalence ratio Φ=0.8, it is about 2800 ppm. From 6%vol of CO_2 in the oxidizer, the emissions of CO are approaching a constant value and tend to stabilize. This increase is expected because the formation of CO is favoured

when the concentration of oxygen is low, when the concentration of the fuel is high and also when the temperature is low, which slows down the reaction rates of oxidation of CH_4 and formation of CO to CO_2 (Erete et al., 2017). To complete these results, CO emissions as a function of CO_2 dilution rate are measured for the swirl number of 1.4 and 0.8, as shown in Figure 16. For all dilution rates, CO emissions for Sn=1.4 are slightly higher than those of Sn= 0.8. CO emissions as a function of O_2 are also measured, in the case of $\phi = 1$ and three swirl numbers (Sn=0.8, 1.1 and 1.4), as shown in Figure17. In the case of the stoichiometric case (Φ=1), CO emissions decrease strongly with oxygen enrichment, but it has the same evolution for all swirl numbers. Depending on the global equivalence ratio, CO emissions may therefore behave differently, as demonstrated by comparing Figure14 and Figure17.

In Figure 18, the combined effects of O_2 enrichment and CO_2 dilution rates on NOx and CO are shown. This makes it possible to identify the optimum conditions in terms of CO and NOx pollutant emissions. These results concern 0% and 10% of CO_2 for 21 to 35% of O_2 enrichment in the case of the swirl number Sn=0.8 and the equivalence ratio Φ=0.8. Without CO_2 dilution, the optimum point corresponds to the 25% of O_2 enrichment. With 10% of CO_2 dilution the optimum point is located at 30% of O_2 enrichment. Depending on the dilution rate, the O_2 enrichment rate is therefore different to obtain the optimum conditions in terms of pollutant emissions. These results indicate that the optimum NOx-CO emissions are linked to the two parameters, CO_2 rate and O_2 rate added.

4. Conclusion

The effects of CO_2 recirculation and air oxygen-enrichment on swirled turbulent methane-air flames are investigated. The configuration of the burner used is coaxial with a swirler in the annular part for the oxidizer supply and a radial injection of methane. The influence of oxygen enrichment (from 21 to 35%) and CO_2 dilution (0 to 16%) on flame stability and

pollutant emissions (NOx and CO) are examined. Effects of global equivalence ratio at the injection (0.8 to 1) and different swirl numbers (0.8, 1.1 and 1.4) are analysed. The OH* chemiluminescence measurements and combustion gases analysis are performed for ~~the~~ different operation conditions.

The main experimental results are:

- Oxygen enrichment leads to a better flame stability, a reduction in the lift-off heights and flame length. The flame becomes more intense and more compact.
- For pollutant emissions, the addition of O_2 in air induces a significant reduction of CO, and an increase in NOx.
- CO_2 dilution in the oxidizer significantly changes the shape and features of the flame. The flame becomes longer, less intense and less stable.
- The addition of CO_2 leads to an increase in CO and a significant reduction of NOx, with a reduction in combustion gases temperature which is due to reduced flame temperature.

- The combined results of CO_2 dilution and O_2 enrichment on CO and NOx emissions perform the optimum points in terms of pollutant emissions. This reveals that the optimum conditions in terms of pollutant emissions (CO and NOx) depend significantly on both dilution rate and oxygen enrichment.

Acknowledgements

This work is supported by the ANR (Agence Nationale de la Recherche), the CNRS and the University of Orléans. The help and useful discussions with Marc MORLAT from the University of Orleans are gratefully acknowledged.

References

Abdul-Wahab, S.A., Charabi, Y., Al-Maamari, R., Al-Rawas, G.A., Gastli, A. and Chan, K. 2015. CO2 greenhouse emissions in Oman over the last forty-two years: Review. *Renewable and Sustainable Energy Reviews*, 52, pp. 1702–1712.

Allouis, C. and Chiariello, F. 2016. Effect on O2 enrichment and CO2 dilution on rapeseed oil combustion in a stationary burner. *Experimental Thermal and Fluid Science*, 73, pp. 49–55.

Boushaki, T., Merlo, N., Chauveau, C. and Gökalp, I. 2017. Study of pollutant emissions and dynamics of non-premixed turbulent oxygen enriched flames from a swirl burner. *Proceedings of the Combustion Institute*, 36 (3), pp. 3959–3968.

Boushaki, T., Sautet, J.-C. and Labegorre, B. 2009. Control of flames by tangential jet actuators in oxy-fuel burners. *Combustion and Flame*, 156 (11), pp. 2043–2055.

Ding, M. G, Du, Z. 1995. Energy & environmental benefits of oxy-fuel combustion. Energy *Environ., Proc. Int. Conf*; pp. 674-684.

Erete, J.I., Hughes, K.J., Ma, L., Fairweather, M., Pourkashanian, M. and Williams, A. 2017. Effect of CO2 dilution on the structure and emissions from turbulent, non-premixed methane–air jet flames. *Journal of the Energy Institute*, 90 (2), pp. 191–200.

European commission. 2006. Integrated pollution prevention and control, Reference document on best available techniques for large combustion plants;.

Favre, E., Bounaceur, R. and Roizard, D. 2009. A hybrid process combining oxygen enriched air combustion and membrane separation for post-combustion carbon dioxide capture. *Separation and Purification Technology*, 68 (1), pp. 30–36.

Gotoh O, Otobe Y, Kawamoto M, Fujimura A. 1984. Exhaust gas recirculation control system for vehicle engines. Japan assigned to Honda Giken Kogyo Kabushiki Kaisha. 10(4).

Honoré D. 2007. Advanced measurements in industrial combustion systems., VKI Lecture Series .Turbulent Combustion, ed Vervisch L, Veynante D, Van Beeck J.P.A.J. Belgium.

Jaramillo, P., Griffin, W.M. and Matthews, H.S. 2007. Comparative Life-Cycle Air Emissions of Coal, Domestic Natural Gas, LNG, and SNG for Electricity Generation. *Environmental Science & Technology*, 41 (17), pp. 6290–6296.

Jerzak, W. and Kuźnia, M. 2016. Experimental study of impact of swirl number as well as oxygen and carbon dioxide content in natural gas combustion air on flame flashback and blow-off. *Journal of Natural Gas Science and Engineering*, 29, pp. 46–54.

Jourdaine, P., Mirat, C., Caudal, J., Lo, A. and Schuller, T. 2016. A comparison between the stabilization of premixed swirling CO2-diluted methane oxy-flames and methane/air flames. *Fuel* [Internet], Available from http://linkinghub.elsevier.com/retrieve/pii/S0016236116311061 [Accessed 22nd February 2017].

Kim, M.-K., Yoon, J., Park, S., Lee, M.-C. and Youngbin Yoon 2013. Effects of unstable flame structure and recirculation zones in a swirl-stabilized dump combustor. *Applied Thermal Engineering*, 58 (1-2), pp. 125–135.

Kim, T.H., Park, J.W., Park, H.Y., Park, J., Park, J.H. and Lim, I.G. 2016. Chemical and radiation effects on flame extinction and NOx formation in oxy-methane combustion diluted with CO2. *Fuel*, 177, pp. 235–243.

Lashof, D.A. and Ahuja, D.R. 1990. Relative contributions of greenhouse gas emissions to global warming. *Nature*, 344 (6266), pp. 529–531.

Lieuwen, T. and Zinn, B.T. 1998. The role of equivalence ratio oscillations in driving combustion instabilities in low NOx gas turbines. *Symposium (International) on Combustion*, 27 (2), pp. 1809–1816.

Liu, F., Karataş, A.E., Gülder, Ö.L. and Gu, M. 2015. Numerical and experimental study of the influence of CO2 and N2 dilution on soot formation in laminar coflow C2H4/air diffusion flames at pressures between 5 and 20atm. *Combustion and Flame*, 162 (5), pp. 2231–2247.

Ma, T. and Takeuchi, K. 2017. Technology choice for reducing emissions: An empirical study of Chinese power plants. *Energy Policy*, 102, pp. 362–376.

Merlo, N., Boushaki, T., Chauveau, C., de Persis, S., Pillier, L., Sarh, B. and Gökalp, I. 2013. Experimental Study of Oxygen Enrichment Effects on Turbulent Non-premixed Swirling Flames. *Energy & Fuels*, 27 (10), pp. 6191–6197.

Merlo, N., Boushaki, T., Chauveau, C., Persis, S.D., Pillier, L., Sarh, B. and Gökalp, I. 2014. Combustion characteristics of methane–oxygen enhanced air turbulent non-premixed swirling flames. *Experimental Thermal and Fluid Science*, 56, pp. 53–60.

Min, J. and Baillot, F. 2012. Experimental investigation of the flame extinction processes of nonpremixed methane flames inside an air coflow diluted with CO2, N2, or Ar. *Combustion and Flame*, 159 (12), pp. 3502–3517.

Nada, Y., Matsumoto, K. and Noda, S. 2014. Liftoff heights of turbulent non-premixed flames in co-flows diluted by CO2/N2. *Combustion and Flame*, 161 (11), pp. 2890–2903.

Nemitallah, M.A. and Habib, M.A. 2013. Experimental and numerical investigations of an atmospheric diffusion oxy-combustion flame in a gas turbine model combustor. *Applied Energy*, 111, pp. 401–415.

Oh, J. and Noh, D. 2014. The effect of CO2 addition on the flame behavior of a non-premixed oxy-methane jet in a lab-scale furnace. *Fuel*, 117, pp. 79–86.

Poinsot, T. 2017. Prediction and control of combustion instabilities in real engines. *Proceedings of the Combustion Institute*, 36 (1), pp. 1–28.

Rashwan, S.S., Ibrahim, A.H., Abou-Arab, T.W., Nemitallah, M.A. and Habib, M.A. 2016. Experimental investigation of partially premixed methane–air and methane–oxygen flames stabilized over a perforated-plate burner. *Applied Energy*, 169, pp. 126–137.

Samaniego, J.M., Labégorre, B., Egolfopoulos, F.N., Ditaranto, M., Sautet, J.C. and Charon, O. 1998. Mechanism of nitric oxide formation in oxygen-natural gas combustion. *Symposium (International) on Combustion*, 27 (1), pp. 1385–1392.

Telesca, A., Marroccoli, M., Ibris, N., Lupiáñez, C., Díez, L.I., Romeo, L.M. and Montagnaro, F. 2017. Use of oxyfuel combustion ash for the production of blended cements: A synergetic solution toward reduction of CO2 emissions. *Fuel Processing Technology*, 156, pp. 211–220.

Wang, S., Ji, C., Zhang, B., Cong, X. and Liu, X. 2016. Effect of CO2 dilution on combustion and emissions characteristics of the hydrogen-enriched gasoline engine. *Energy*, 96, pp. 118–126.

Wei, Z.L., Leung, C.W., Cheung, C.S. and Huang, Z.H. 2016. Effects of equivalence ratio, H2 and CO2 addition on the heat release characteristics of premixed laminar biogas-hydrogen flame. *International Journal of Hydrogen Energy*, 41 (15), pp. 6567–6580.

Wu, K.-K., Chang, Y.-C., Chen, C.-H. and Chen, Y.-D. 2010. High-efficiency combustion of natural gas with 21–30% oxygen-enriched air. *Fuel*, 89 (9), pp. 2455–2462.

Yap, L.T., Pourkashanian, M., Howard, L., Williams, A. and Yetter, R.A. 2008. Nitric-Oxide Emissions Scaling of Buoyancy-Dominated Oxygen-Enriched Methane Turbulent-Jet Diffusion Flames. In: Saito, K. ed. *Progress in Scale Modeling*. [Internet] Dordrecht, Springer Netherlands, pp. 203–209. Available from http://link.springer.com/10.1007/978-1-4020-8682-3_16 [Accessed 1st June 2017].

Yu, B., Lee, S. and Lee, C.-E. 2015. Study of NOx emission characteristics in CH4/air non-premixed flames with exhaust gas recirculation. *Energy*, 91, pp. 119–127.

Table 1

Operating conditions: equivalence ratio, swirl number, % of CO_2 and O_2, flow rates of air, O_2, CO_2 and CH_4, bulk velocity of CH_4 and oxidizer.

	% vol	Q_{air} (NL/min)	Q_{O_2} (NL/min)	Q_{CO_2} (NL/min)	Q_{CH_4} (NL/min)	V_{CH_4} (m/s)	V_{oxid} (m/s)
ϕ =0.8	For three swirl numbers, Sn : 0.8 , 1.1 and 1.4						
O_2 enrichment	21	150	0	0	12.6	3.99	2.80
	25	142	7.57	0	14.95	4.73	2.79
	30	133	17.1	0	18.01	5.70	2.80
CO_2 dilution	4	144	0	5.76	12.09	3.83	2.79
	8	139	0	11.12	11.67	3.69	2.80
	12	134	0	16.08	11.25	3.56	2.80
ϕ=0.9	For three swirl numbers, Sn : 0.8 , 1.1 and 1.4						
O_2 enrichment	21	150	0	0	14.17	4.48	2.80
	25	142	7.57	0	16.82	5.32	2.79
	30	133	17.1	0	20.26	6.41	2.80
CO_2 dilution	4	144	0	5.76	13.608	4.3	2.79
	8	139	0	11.12	13.13	4.15	2.80
	12	134	0	16.08	12.66	4.01	2.80
ϕ=1	For three swirl numbers, Sn : 0.8 , 1.1 and 1.4						
O_2 enrichment	21	150	0	0	15,75	4.98	2.80
	25	142	7.57	0	18.69	5.91	2.79
	30	133	17.1	0	22.51	7.12	2.80
CO_2 dilution	4	144	0	5.76	15,12	4.78	2.79
	8	139	0	11.12	14.59	4.62	2.80
	12	134	0	16.08	14.07	4.45	2.80

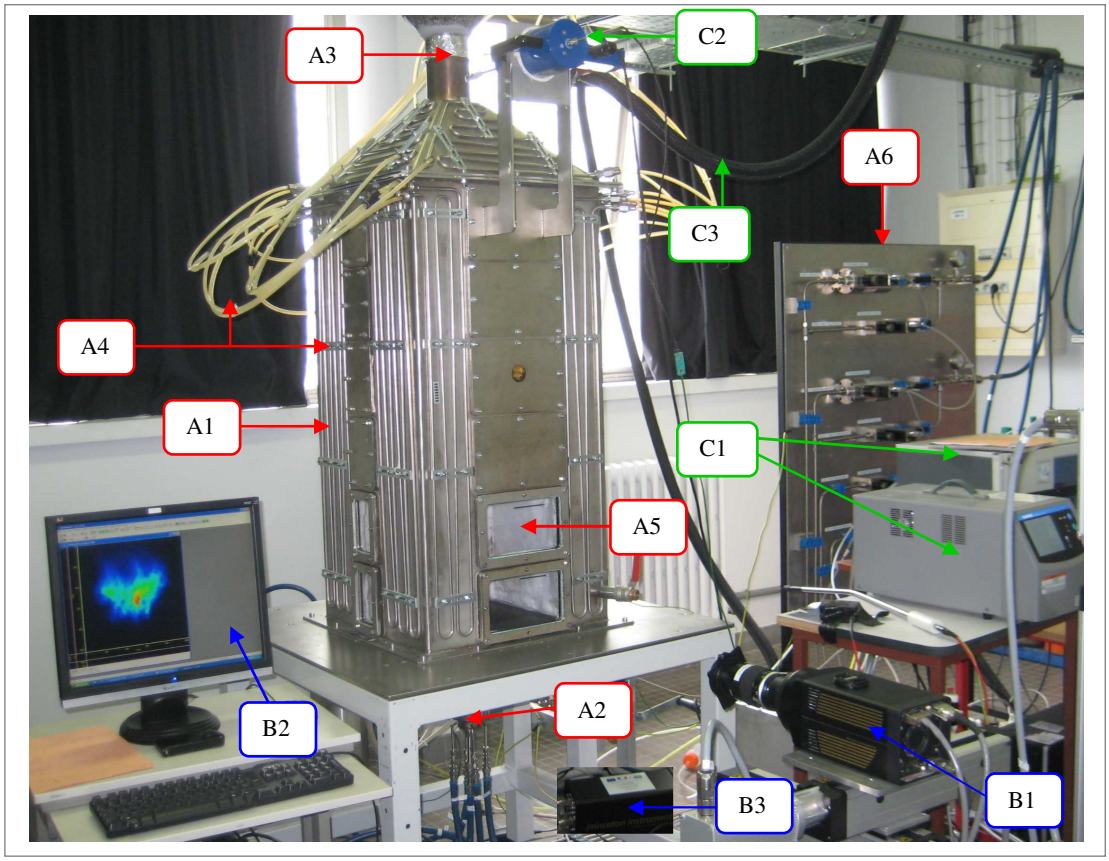

Figure 1. Experimental facility: combustion chamber (Ai, A1: combustion chamber, A2: coaxial burner, A3: extraction tube, A4: cooling water system, A5: windows of visualization, A6: gas supply panel), chemiluminescence system (Bi, B1: ICCD camera, B2: computer, B3: camera intensifier) and gas analyzers with sampling probe (Ci, C1: gas analysers, C2: sampling probe (PSP4000-HCT), C3: heated gas transport line).

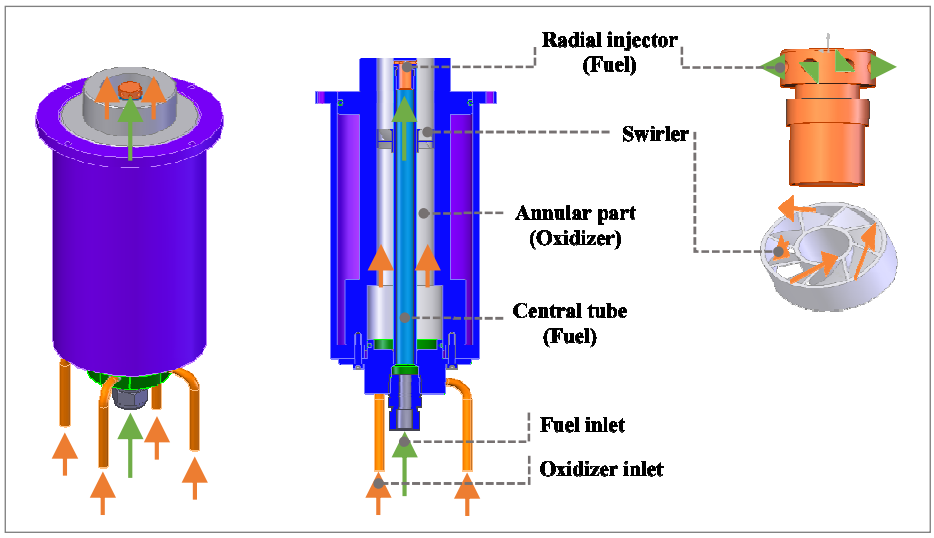

Figure 2. Coaxial burner diagram

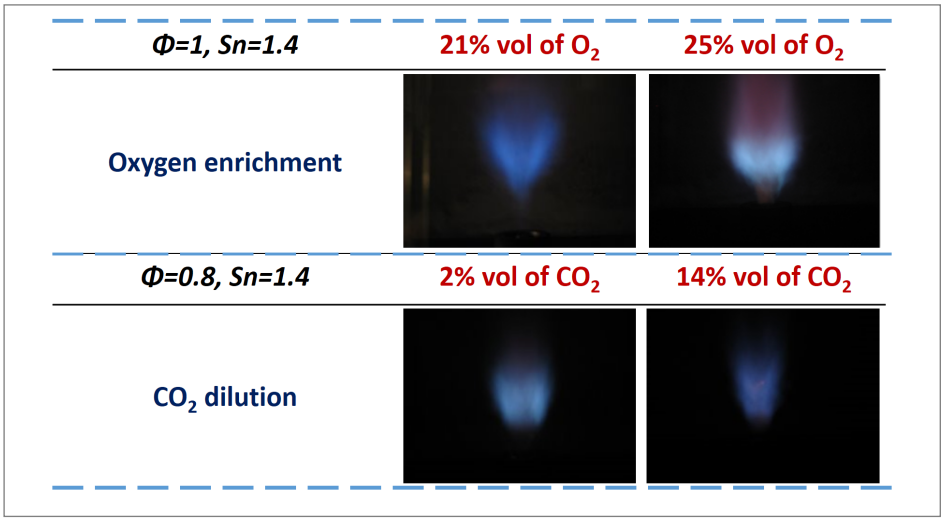

Figure 3. Examples of flame images with oxygen enrichment (top) and CO_2 dilution (bottom)

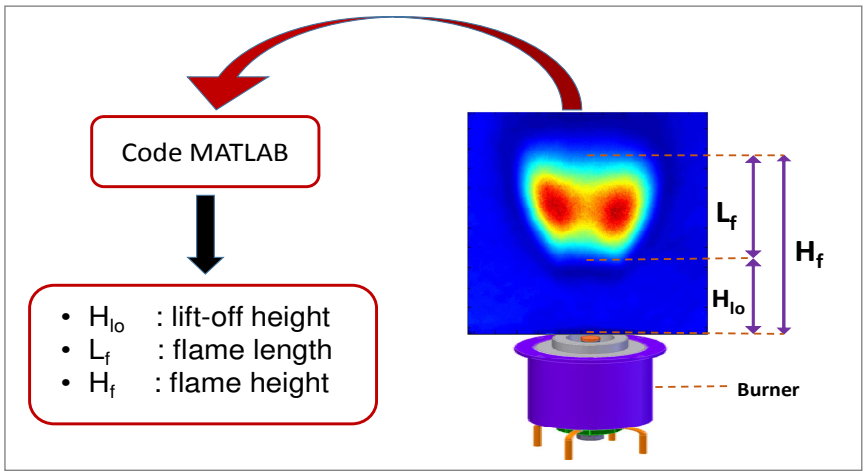

Figure 4. Descriptive diagram of lift-off height, flame length and flame height

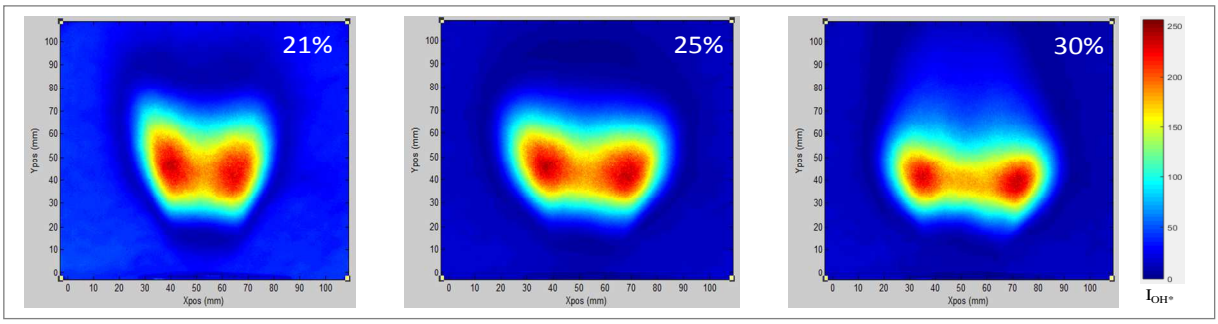

Figure 5. Average images of OH* chemiluminescence without O_2 enrichment (21%) and with enrichment (25 and 30%) for Sn=1.4, ϕ = 0.8 and 10%vol of CO_2 in the oxidizer.

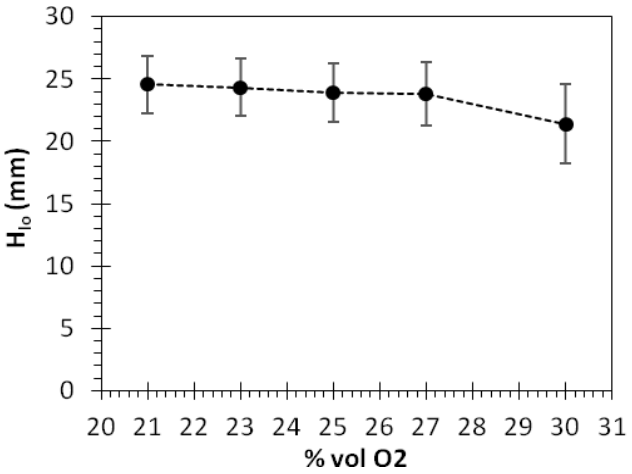

Figure 6. Lift-off height with oxygen enrichment for ϕ = 0.8, Sn = 1.4 and 10%vol of CO_2 in the oxidizer.

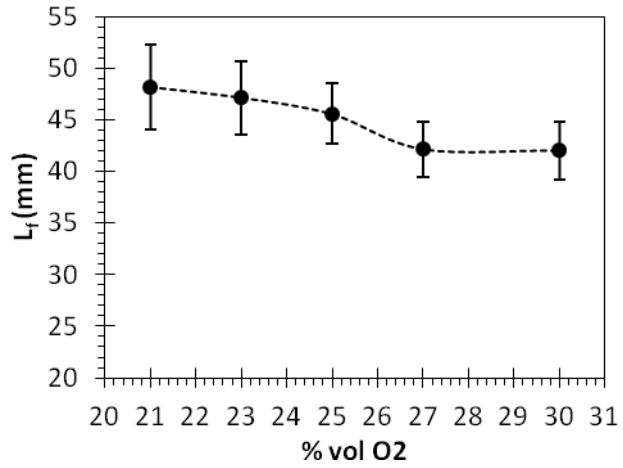

Figure 7. Flame length with oxygen enrichment for ϕ = 0.8, Sn = 1.4 and 10 % vol of CO_2 in the oxidizer.

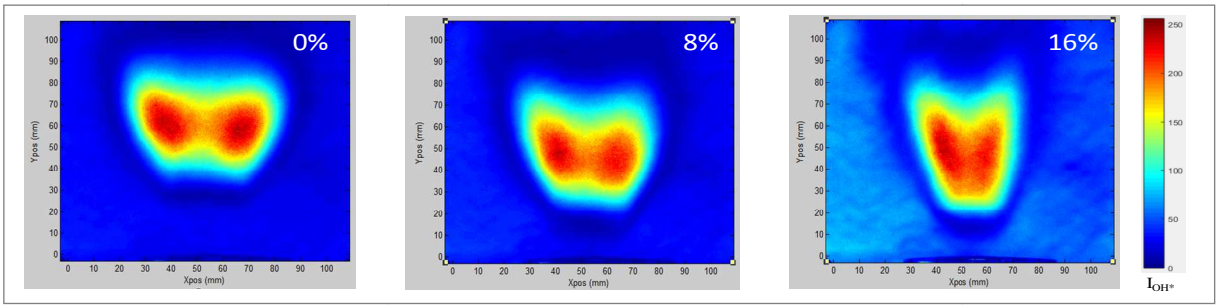

Figure 8. Average images of OH* chemiluminescence without CO_2 dilution (0% of CO_2) and with CO_2 dilution (8 and 16%) for Sn = 1.4 and ϕ = 0.8.

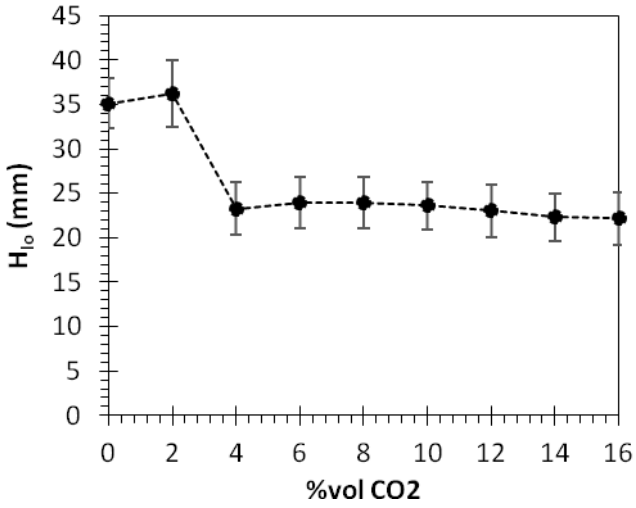

Figure 9. Lift-off height with CO_2 dilution for ϕ = 0.8, Sn = 0.8 and 21%vol of O_2 in the oxidizer.

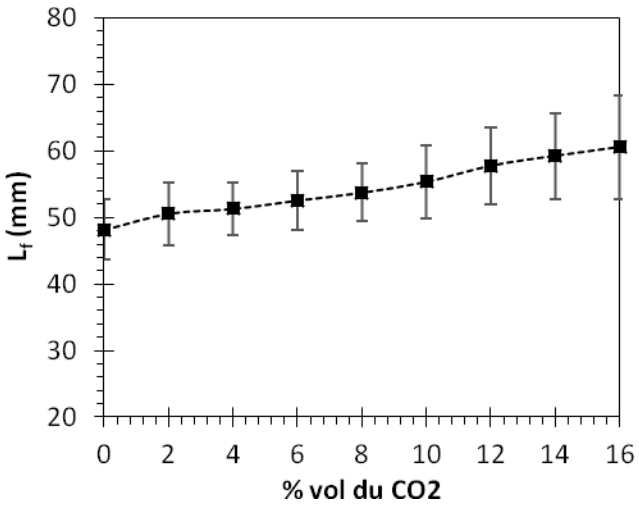

Figure 10. Flame length with CO_2 dilution for Sn = 1.4, ϕ = 0.8 and 21%vol of O_2 in the oxidizer.

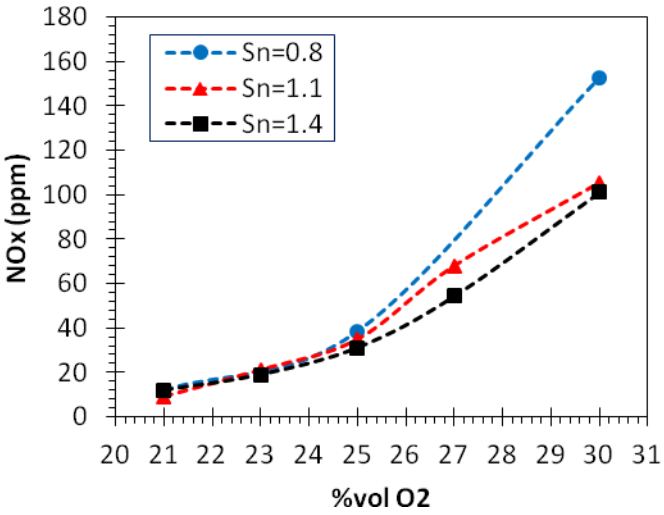

Figure 11. NOx emissions with O_2 enrichment at ϕ=1 for three swirl numbers 0.8, 1.1 and 1.4.

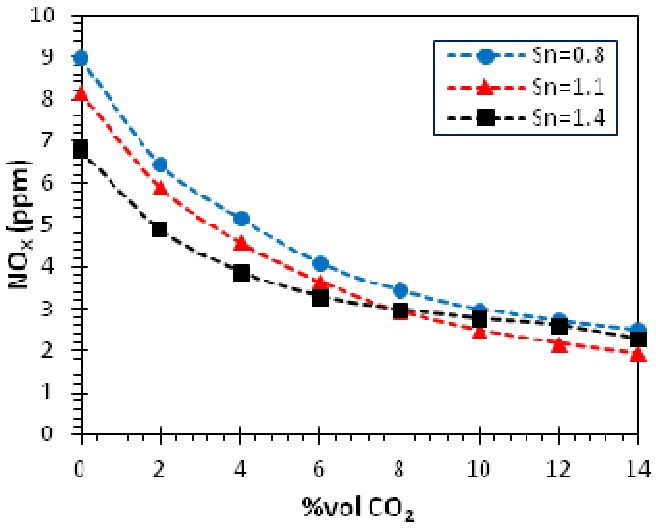

Figure 12. NOx emissions with CO_2 dilution at ϕ = 0.8 and 21%vol of O_2 for three swirl numbers 0.8, 1.1 and 1.4.

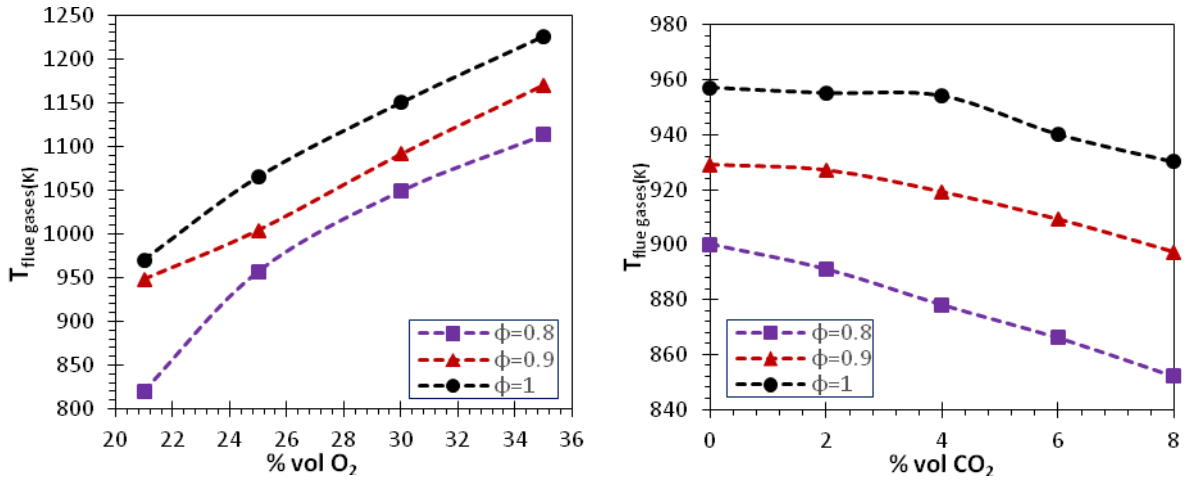

Figure 13. Temperatures of flue gases with O_2 enrichment (left) and CO_2 dilution (right) for Sn=0.8 at three equivalence ratios ϕ=0.8, 0.9 and 1.

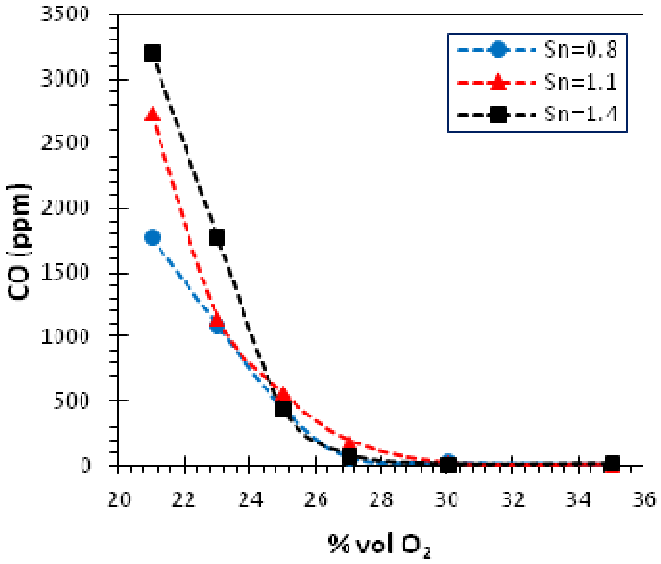

Figure 14. CO emissions with O_2 enrichment at ϕ = 0.8 for three swirl numbers 0.8, 1.1 and 1.4.

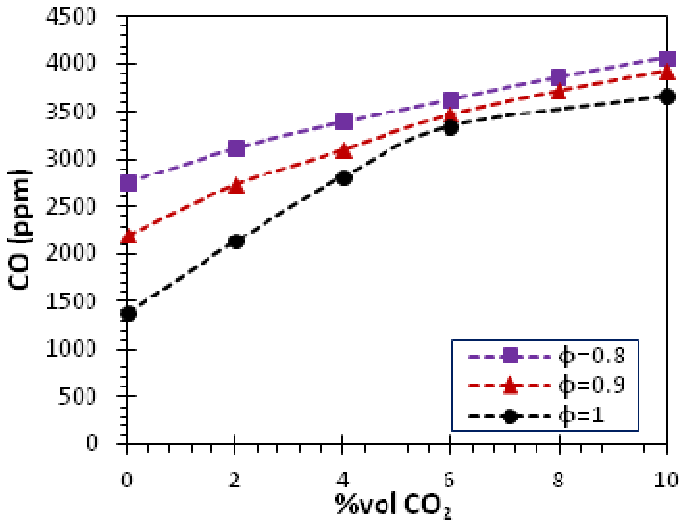

Figure 15. CO emissions with CO_2 dilution for Sn = 0.8 and 21%vol of O_2 at three different equivalence ratios ϕ=0.8, 0.9 and 1.

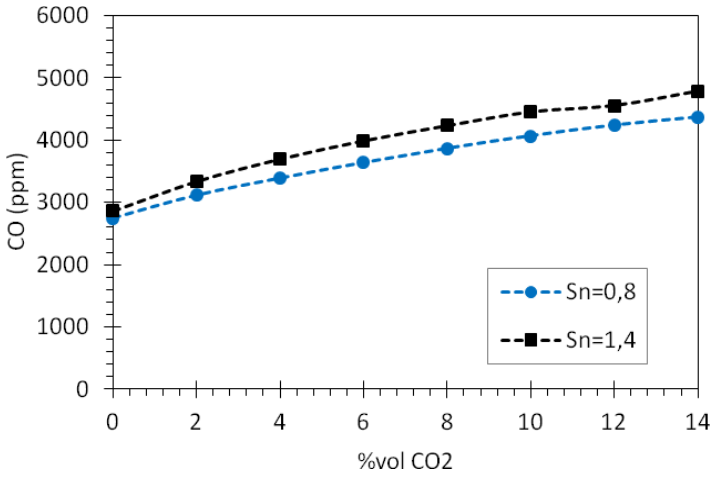

Figure 16. CO emissions with CO_2 dilution at ϕ =0.8, 21% of O2, and for Sn= 0.8 and 1.4.

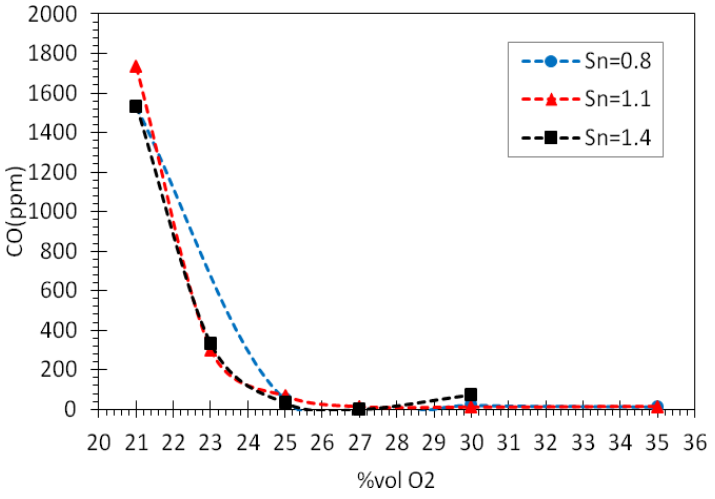

Figure 17. CO emissions with O_2 enrichment at ϕ = 1 for three swirl numbers 0.8, 1.1 and 1.4.

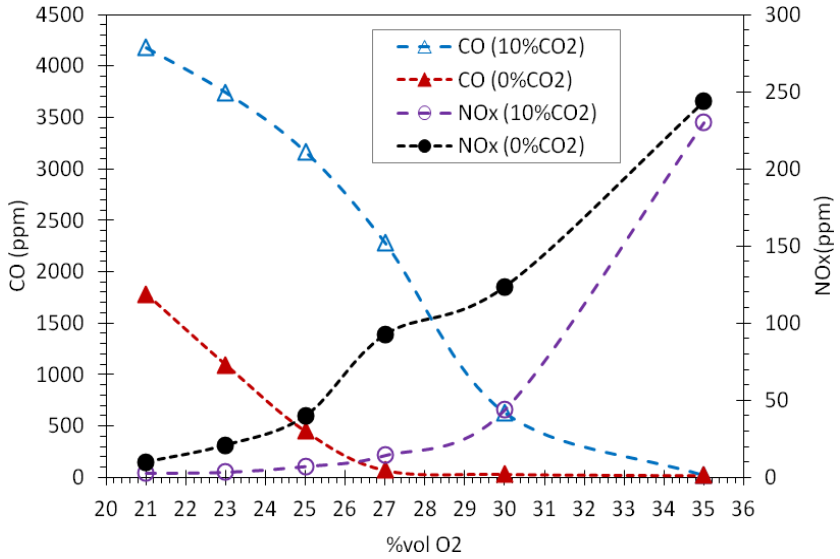

Figure 18. Combination of NOx and CO emissions with CO_2 dilution for 21 and 25% of O_2 enrichment, in the case of Sn=1.4 and ϕ = 0.8.